Inhibiting Performance of Rivaroxaban Against Corrosion of Mild Steel in 1.0 M HCl Solution

H. Ashassi-Sorkhabi*, M. Mehralizadeh and E. Asghari

Electrochemistry Research Laboratory, Department of Physical Chemistry, Faculty of Chemistry, University of Tabriz, Tabriz, Iran

(Received 10 August 2023, Accepted 1 November 2023)

Before being used in a variety of sectors, steel is often cleaned using acidic solutions. The steel corrosion rises because of this treatment, necessitating the inclusion of inhibitors in the cleaning bath. Due to this, it is constantly crucial to provide new and effective corrosion inhibitors. Rivaroxaban was investigated in this study as a mild steel corrosion inhibitor in a 1.0 M HCl solution. Corrosion experiments were conducted using potentiodynamic polarization and electrochemical impedance spectroscopy (EIS). The considered temperatures were 25 °C, 30 °C, 40 °C, and 50 °C, and concentrations of the inhibitor were 1, 10, 20, 30, and 40 µM. Steel sheets' surfaces were analyzed using SEM images in both the absence and presence of the inhibitor. At an ideal concentration of 40 µM, Rivaroxaban demonstrated inhibition efficiency greater than 92%, which was reduced with an increase in temperature and time of immersion in the acidic solution. Charge transfer resistance in the presence of Rivaroxaban after 144 h decreased from 1470 to 231 Ω cm^2.
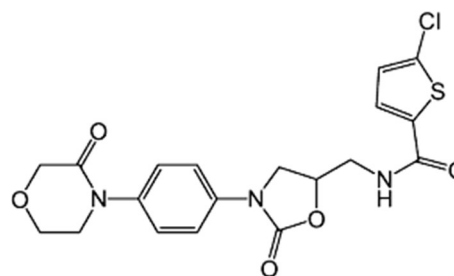
Keywords: Rivaroxaban, Corrosion inhibitor, Mild steel, EIS, polarization

INTRODUCTION

There are several industrial applications for mild steel. Acidic solutions are often utilized in the majority of industrial operations for pickling, industrial acid cleaning, acid descaling, and oil well acidifying [1-4]. Before its use, mild steel (MS) is frequently cleaned by acid pickling. Steel, however, corrodes too readily in acidic solutions and is hence susceptible to rusting. Inhibitors can be used to effectively slow down the corrosion of steel. Moreover, applying additional techniques, such protective coatings, is thought to be another effective strategy for steel protection [5-14]. The easiest method for reducing metal dissolving in pickling solutions is to utilize inhibitors. In this framework, it has been claimed that organic molecules containing heteroatoms like oxygen and nitrogen, as well as π-electrons in conjugated double and triple bonds, work effectively as corrosion inhibitors [15-24].

Rivaroxaban, because of its chemical structure, which contains a lot of oxygen and nitrogen atoms, can function as active sites for effective adsorption on the metal surface.

Furthermore, it offers an adequate source of π-electrons, which increases the electron donating tendency toward the proper unoccupied d-orbital of the steel, resulting in the formation of an adsorption layer [25]. The inhibition efficiency depends on the type of heteroatoms so that oxygen, nitrogen, and sulfur follow the order S > O > N to increase the inhibition ability [12,26,27]. According to Scheme 1, Rivaroxaban contains all the above-mentioned groups that were effective in corrosion inhibition.

Scheme 1. Chemical structure of 4-{4-[(5S)-5-(aminomethyl)-2-oxo-1,3-oxazolidin-3-yl]phenyl}morpholin-3-one (Rivaroxaban)

All these factors make Rivaroxaban a suitable choice for use as a mild steel corrosion inhibitor. On this basis, the potential of Rivaroxaban to reduce steel corrosion was examined in the current investigation using electrochemical methods. The aim of this work is to investigate the inhibition effectiveness of Rivaroxaban on the mild steel corrosion in 1.0 M HCl solution. The effects of temperature and concentration on the inhibition efficiency were compared. The results showed that the suggested compound might be employed as an effective MS inhibitor in acidic media.

EXPERIMENTAL

Rivaroxaban was purchased from Actoverco pharmaceutical company, and hydrochloric acid (37%) was bought from Merck. The steel sheets' composition was (in weight percent) Mn 0.260, C 0.008, Ni 0.016, Si 2.08, Cr 0.034, Mo 0.018, Al 0.353, S 0.005, W 0.014, and Ti 0.007. A three-electrode cell connected to an Autolab PGSTAT30 Potentiostat-Galvanostat was used for the electrochemical testing. The MS sheets used to create the working electrode were mounted by polyester so that a 1 cm^2 region was exposed to the solution then were polished with SiC papers and finally degreased. The counter electrode was a platinum sheet, and the reference electrode was Ag/AgCl (3 M KCl). EIS measurement was made in a frequency range of 1×10^5 0.01 Hz, and potentiodynamic polarization (PDP) measurement was carried out in a potential range of -250-250 mV *versus* open circuit potential at a scan rate of 1 mV s^{-1}. The linear parts of the obtained Tafel diagrams were analyzed by NOVA software. The temperature of the cell holder was maintained at a consistent level by a thermostatically regulated bath, enabling electrochemical experiments at various temperatures. MIRA3 FEG Tescan Field emission scanning electron microscope (FE-SEM) was used to analyze the steel surface before and after exposure to the acidic environment.

RESULTS AND DISCUSSION

EIS Analysis

EIS measurements were made for mild steel in the absence and presence of various concentrations of Rivaroxaban (1, 10, 20, 30, and 40 μM) at 25 °C. For the
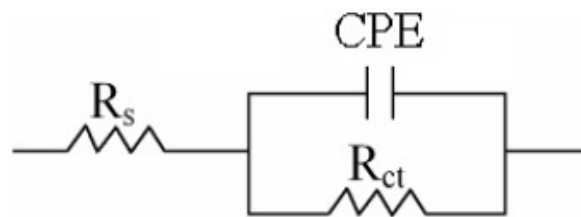

Fig. 1. Equivalent circuit used for fitting the measured EIS data.

best inhibitor concentration, tests were also made at various temperatures of 25 °C, 30 °C, 40 °C, and 50 °C.

The equivalent circuit depicted in Fig. 1 was used to examine the data that was acquired. R_s stands for the solution resistance in this circuit, R_{ct} is the corrosion resistance or charge transfer resistance, and CPE_{dl} is the constant phase element of double layer.

Table 1 provides the final EIS parameters for each concentration of the inhibitor. The values of inhibition efficiency (η_z) and capacitance of the double layer (C_{dl}) generated at the metal/electrolyte interface were calculated using the following formulae [28,29]:

$$\eta\% = \frac{R_{ct} - R_{ct}^0}{R_{ct}} \times 100 \tag{1}$$

$$C_{dl} = (R_{ct}^{1-n} \times Y_0)^{1/n} \tag{2}$$

Here, R_{ct} and R_{ct}^0 are charge transfer resistance when the inhibitor is present and absent, respectively.

Figure 2 shows the MS Nyquist diagrams in 1.0 M HCl solution with and without Rivaroxaban. In Nyquist plots, the semicircle diameter is known as R_{ct}, and it is inversely proportional to the corrosion rate. Figure 2 demonstrated that the diameter of the capacitive loops grew as the concentration of Rivaroxaban in the solution increased, indicating that the inhibitor concentration affected the inhibitor efficacy. At larger concentrations, more inhibitor molecules were deposited on the surface, which could increase corrosion resistance. Additionally, it is clear from Nyquist plots that they had the shape of a single capacitive loop both in the absence and presence of the inhibitor, showing that the addition of Rivaroxaban had no effect on the mechanism of

Table 1. EIS Parameters Obtained for Mild Steel in 1.0 M HCl Solution in the Absence and Presence of Various Concentrations of Rivaroxaban at Different Temperatures and Immersion Times

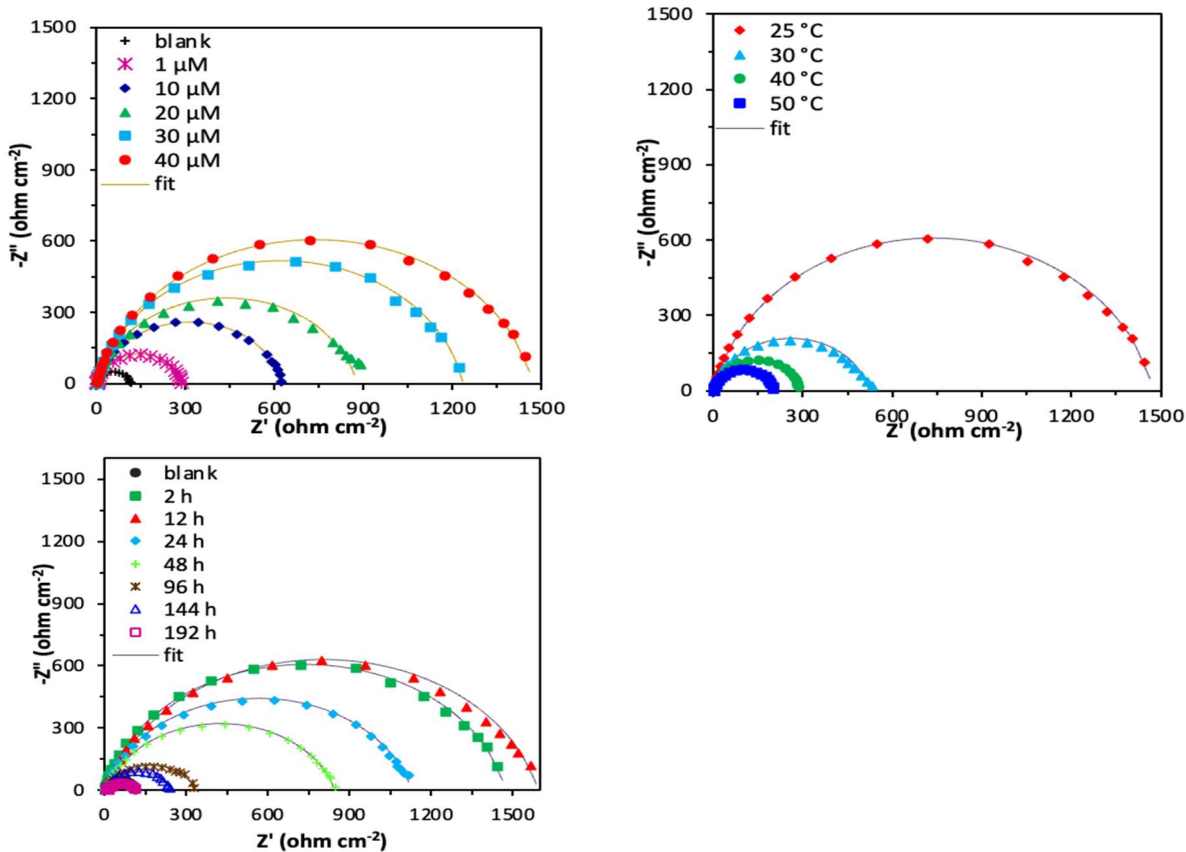| Immersion time (h)	T (ºC)	C_{inh} (µM)	CPE_{dl} $Y_0 \times 10^{-6}$ (Ω^{-1} cm^{-2} S^n)	n	R_{ct} (Ω cm^2)	C_{dl} (µF cm^{-2})	η_z (%)	Fitting error
2	25	0	106.120	0.91	113	68.52	-	0.0030
2	25	1	80.156	0.91	281	54.91	59.79	0.0001
2	25	10	61.868	0.91	622	47.64	81.83	0.0005
2	25	20	57.080	0.87	872	46.49	87.04	0.0035
2	25	30	62.554	0.89	1230	45.39	90.81	0.0019
2	25	40	61.494	0.88	1470	44.31	92.31	0.0048
2	30	40	77.984	0.86	522	46.31	78.35	0.0013
2	40	40	80.703	0.89	286	50.65	60.49	0.0005
2	50	40	73.705	0.88	200	41.47	43.50	0.0003
12	25	40	59.887	0.86	1580	40.80	92.85	0.0032
24	25	40	68.441	0.85	1125	43.53	89.96	0.0040
48	25	40	80.644	0.83	844	46.51	86.61	0.0020
96	25	40	170.160	0.77	322	71.47	64.91	0.0013
144	25	40	181.190	0.74	231	74.84	51.08	0.0080
192	25	40	932.760	0.69	111	180.53	-1.80	0.0016

Fig. 2. Effects of concentration of Rivaroxaban, temperature, and immersion time on the EIS diagrams of mild steel in 1.0 M HCl solution. The inhibitor concentration ranges from 1 to 40 µM, where 40 µM was defined as the optimum content and selected for investigating the temperature influence on the inhibiting properties.

steel corrosion. According to the data in Table 1, C_{dl} had a value of 68.52 mF cm^{-2} for MS in the blank solution. However, it showed a decline in the presence of the inhibitor. The reason for this discovery is that the thickness of the electrical double layer was increased because of the Rivaroxaban molecules' adhering to the steel surface. In other words, this is due to the displacement of water molecules onto the mild steel surface by the adsorbed species of the inhibitor, which leads to a decrease in the dielectric constant due to the increase in double layer thickness, thereby protecting the mild steel surface from acid attack. The impact of temperature on the effectiveness of inhibition in the presence of 40 µM Rivaroxaban demonstrated a decrease in inhibition efficiency from 92.31% at 25 °C to 43.50% at 50 °C. This may be caused by an accelerated rate of mild steel dissolving and partial desorption of the inhibitor from the metal surface because of temperature. Furthermore, inhibition efficiency in the presence of 40 µM Rivaroxaban dropped from 92.31% after 2 h of immersion to 51.08% after 144 h of immersion. It was also observed that inhibition efficiency possessed a negative value after 192 h of immersion, indicating that the inhibitory action of Rivaroxaban was lost due to extended exposure to the aggressive environment. The results obtained from EIS measurements indicated that the addition of 40 µM of Rivaroxaban remarkably reduced the MS corrosion, as demonstrated by an increase in the Rct from 1470 to 113 Ω cm2.

Potentiodynamic Polarization Results

Tafel curves recorded for MS in 1.0 M HCl solution with and without Rivaroxaban were used to further investigate the inhibiting effect of the studied inhibitor.

The Tafel plots, shown in Fig. 3, were examined to determine a few crucial parameters, including Tafel slopes (b_a and b_c), corrosion potential (E_{corr}), corrosion current density (i_{corr}), and polarization resistance (R_p), which are shown in Table 2. This table demonstrates how i_{corr} shifted to lower values when the inhibitor was added to the acidic medium, and how this impact was amplified when inhibitor concentration was increased. According to this observation, the suggested compound slows down the rate at which steel dissolves in the HCl solution.

The following equation is used to determine inhibition efficiencies using the obtained i_{corr} values [30].

$$\eta\% = \frac{i_{corr}^0 - i_{corr}}{i_{corr}^0} \times 100 \tag{3}$$

Here, i_{corr}^0 and i_{corr} represent the corrosion current densities in the presence and absence of the inhibitor, respectively.
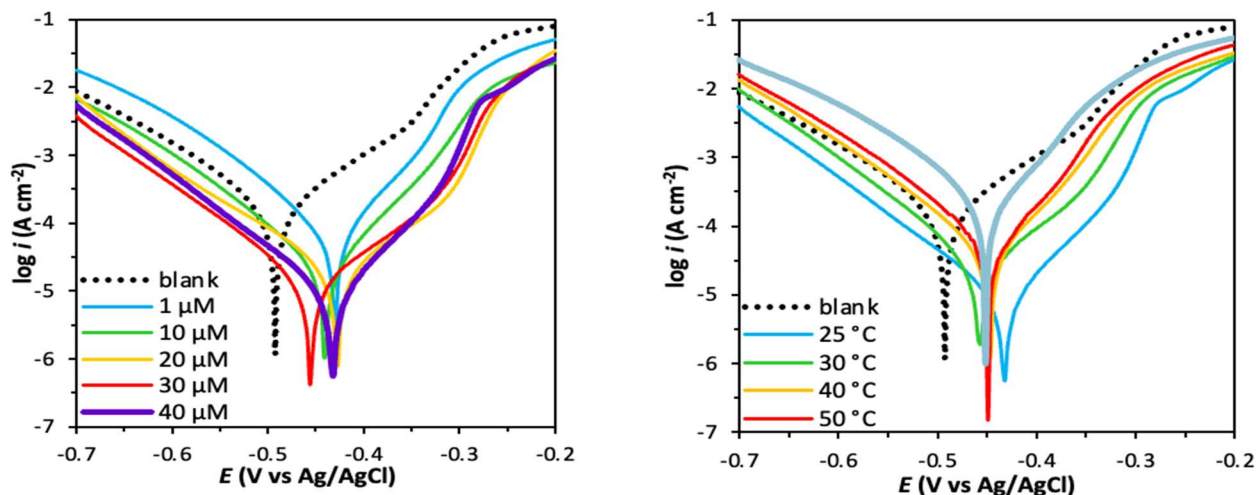

Fig. 3. Effects of concentration of Rivaroxaban and temperature on the Tafel curves of mild steel in 1.0 M HCl solution. The inhibitor concentration ranges from 1 to 40 µM, where 40 µM was defined as the optimum content and selected for investigating the temperature influence on the inhibiting.

Table 2. PDP Parameters Obtained for Mild Steel in 1.0 M HCl Solution in the Absence and Presence of Various Concentrations of Rivaroxaban at Different Temperatures and Immersion Times

T (ºC)	C_{inh} (µM)	E_{corr} (mV $vs.$ Ag/AgCl)	i_{corr} (µA cm^{-2})	b_a (mV dec^{-1})	b_c (mV dec^{-1})	R_p (Ω cm^2)	η_p (%)
25	0	-492.83	124.01	90.56	96.54	163.64	-
25	1	-429.18	52.18	76.32	69.68	303.10	57.91
25	10	-440.31	17.72	82.40	68.31	915.50	85.70
25	20	-427.51	14.82	91.48	88.99	1322.10	88.04
25	30	-455.24	10.74	87.04	101.94	1899.10	91.38
25	40	-432.46	8.08	90.42	75.51	2163.30	93.48
30	40	-457.08	22.21	78.66	93.57	835.68	82.08
40	40	-446.79	33.81	82.02	67.98	477.44	72.73
50	40	-448.65	42.80	81.82	64.65	366.45	65.48

Table 2 provides the obtained values of inhibition efficiency. Compared to an inhibited solution, the MS inhibition efficiency in the blank solution is substantially lower. Additionally, when the inhibitor concentration increased, inhibition efficiency increased as well. Table 2 demonstrated that the R_p values increase at greater concentrations. This observation was corroborated by a decreasing trend for the i_{corr} values at concentrated solutions, which showed that the protective layer was expanding as the inhibitor content enhanced. Accordingly, if the shift is more than 85 mV, inhibitors are classed as anodic or cathodic type; otherwise, they may be classified as mixed type. According to Table 2, none of the shifts in E_{corr} was more than 85 mV, which points to a mixed-type inhibition mechanism. This indicated that the inhibitor had an impact on both the hydrogen evolution and the dissolution of steel, as seen by a simultaneous alteration in the anodic and cathodic Tafel slopes. By comparing Tafel curves at four temperatures of 25 °C, 30 °C, 40 °C, and 50 °C at the optimal concentration of the inhibitor, the influence of temperature on the corrosion resistance of MS was elucidated. The i_{corr} value was seen to rise from 8.08 µA cm^{-2} at 25 °C to 42.80 µA cm^{-2} at 50 °C, suggesting the occurrence of a more sever steel corrosion at higher temperatures. The reason for this finding was a rise in the corrosive ions' mobility, which made it easier for them to reach the metal surface. The inhibition efficiency in the presence of 40 µM Rivaroxaban was 93.48%. The results

obtained from polarization measurements indicated that the addition of 40 µM of Rivaroxaban remarkably reduced MS corrosion, where polarization resistance became 2163.30 Ω cm^2.

Adsorption Isotherms

Adsorption isotherms provide further details about the potential interactions between the inhibitor and the metal. A relationship between the inhibitor concentration and surface coverage (Θ) is used to determine adsorption isotherms. The Θ data were fitted to several equations, including Temkin, Frumkin, Freundlich, and Langmuir, represented by Eqs. (4) to (7), to select an acceptable isotherm to model the system under study [31].

$$\theta = -\frac{1}{2a}\ln K - \frac{1}{2a}\ln C \tag{4}$$

$$\log \theta = \log K + \frac{1}{n}\log C \tag{5}$$

$$\log \frac{\theta}{1-\theta} = \log K + \log C \tag{6}$$

$$\frac{c}{\theta} = \frac{1}{K} + C \tag{7}$$

Here, C is the inhibitor concentration and K is the equilibrium

constant of adsorption-desorption process. The surface coverage values were calculated using the following relation:

$$\theta = \frac{\eta(\%)}{100} \tag{8}$$

Here, the values of η were taken from Table 2. For the studied isotherms, the fit regression coefficients (R^2) were found. The value of R^2 for the Langmuir equation was closer to one than the other equations. Therefore, the Langmuir isotherm was the model that best described our system. As shown in Fig. 4, the K value can be calculated using the log[θ/(1-θ)] *vs.* logC plot.

The obtained value of K was used to compute the standard Gibbs free energy of adsorption process (ΔG_{ads}^0) by the following equation [31]:

$$\Delta G_{ads}^0 = -RT \ln(55.5K) \tag{9}$$

The values of K and ΔG_{ads}^0 were obtained as 834578.9 M^{-1} and -43.80 kJ mol^{-1}, respectively. K stands for the equilibrium constant of the adsorption-desorption process, and its higher magnitudes may be an indication of large numbers of inhibitor molecules adsorbed on the metal surface. The negative ΔG_{ads}^0 value of the studied system indicates that the adsorption of Rivaroxaban on the steel surface occurs spontaneously. It is commonly accepted that the physical adsorption caused by electrostatic interactions between the charged metal and the inhibitor is dominant if the ΔG_{ads}^0 value is near to -20 kJ mol^{-1} or below. However,
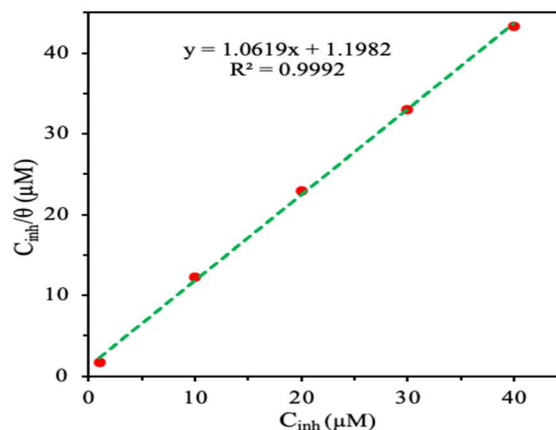

Fig. 4. Langmuir adsorption plot of mild steel in 1.0 M HCl solution containing Rivaroxaban at 25 °C.

chemisorption, which is the outcome of the charge transfer from the inhibitor molecules to the metal surface to create a coordinate kind of bond, is given a value of -40 kJ mol^{-1} or more negative. A mixed-type of adsorption may be implied by the value of ΔG_{ads}^0 between -20 and -40 kJ mol^{-1} [13]. On this basis, the value of -43.80 kJ mol^{-1} obtained for ΔG_{ads}^0 suggested chemisorption for the adsorption process of Rivaroxaban on the steel surface. It should also be mentioned that a potential limitation for application of this inhibitor could be low solubility in acidic media. However, the results obtained here revealed that Rivaroxaban in a low concentration of only 40 μM exhibited a proper inhibition efficiency. The result of corrosion protection of Rivaroxaban was compared with that of literature and the values of them are given in Table 3.

Table 3. Comparison of the Results Obtained in this Work with those Reported in Literature

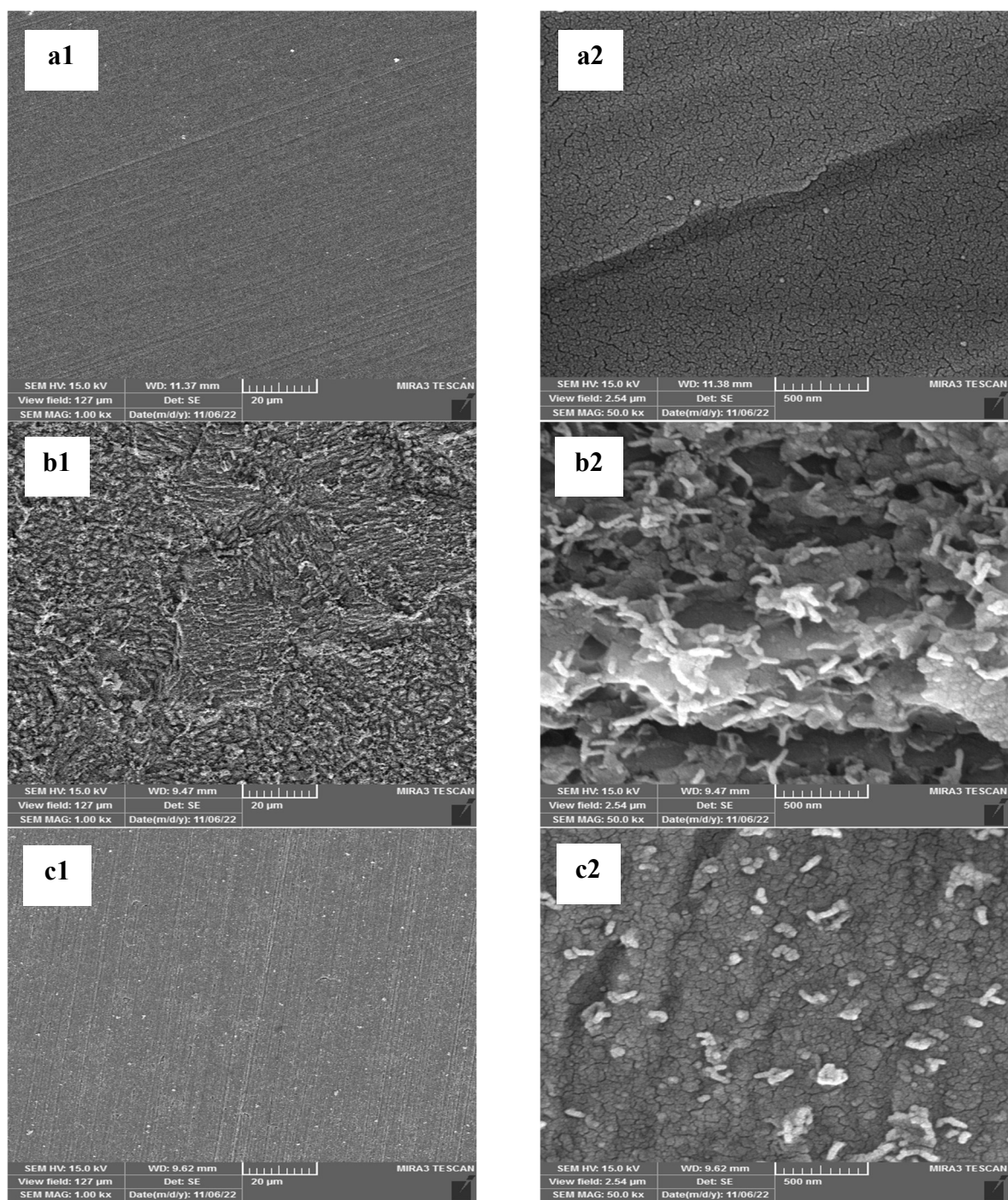| Inhibitors	Substrate	Media	Con.	T (°C)	Immersion time (h)	η (%)	Ref.
Ranitidine	Mild steel	1.0 M HCl	400 ppm	30	6	92	[1]
Tramadol	Mild steel	1.0 M HCl	100 ppm	35	3	97.20	[2]
Lorazepam	Mild steel	3.0 M HCl	0.4 g l^{-1}	30	3	96.49	[3]
Podocip: cefpodoxime proxetil	Carbon steel	1.0 M HCl	100 ppm	35	3	97.93	[4]
Tobramycin	Carbon steel	2.0 M HCl	500 ppm	50	0.5	92.60	[5]
Atorvastatin	Mild steel	1.0 M HCl	150 ppm	25	3	99.08	[6]
Pantoprazole sodium	High carbon steel	1.0 M HCl	300 ppm	25	0.5-3	95.10	[7]
Rivaroxaban	Mild steel	1.0 M HCl	40 μM	25	48	86.61	This work

Fig. 5. SEM images of mild steel before immersion (a), after 24 h immersion in 1.0 M HCl without inhibitor (b), and after 24 h immersion in 1.0 M HCl containing 40 µM inhibitor (c).

Surface Analysis

SEM images were used to examine the morphology of the steel surface in the presence and absence of Rivaroxaban. After 24 h of immersion of the steel sheets in the blank solution and the solution containing 40 µM inhibitor, the SEM images shown in Fig. 5 were obtained. This figure made

it clear that there were no inhibitors present when the steel surface was attacked. While when there was an inhibitor, a protective layer was formed on the surface, which prevented the electrolyte from reaching the metal and the corrosion of the steel was almost stopped (Fig. 5b). The FE-SEM images indicated that in the presence of inhibitor, no significant damages to the surface of MS were observed after 24 h immersion in acidic solution.

CONCLUSION

Rivaroxaban, having heteroatoms and π electrons in its molecular structure, has potential to be used as a corrosion inhibitor. Therefore, this was investigated by electrochemical corrosion tests, including electrochemical. The obtained data showed that the addition of 40-μM rivaroxaban to 1 M HCl solution at room temperature resulted in 92% inhibition for mild steel. This level of inhibition offered by a small quantity of the compound shows its feasibility for practical applications. As expected, the inhibition performance of Rivaroxaban reduced with increasing temperature. Furthermore, inhibition efficiency dropped at longer immersion times, providing evidence that the proposed inhibitor was not suitable for prolonged exposure of the steel to the aggressive medium. The good performance of Rivaroxaban in inhibiting the MS corrosion in HCl solution can make it a proper inhibitor for use in corrosion protection of other metals in different environments.

ACKNOWLEDGMENTS

REFERENCES

[1] Bashir, S.; Thakur, A.; Lgaz, H.; Chung, I. -M.; Kumar, A., Computational and experimental studies on Phenylephrine as anti-corrosion substance of mild steel in acidic medium. *J. Mol. Liq.*, **2019**, *293*, 111539. https://doi.org/10.1016/j.molliq.2019.111539.

[2] Döner, A.; Solmaz, R.; Özcan, M.; Kardaş, G., Experimental and theoretical studies of thiazoles as corrosion inhibitors for mild steel in sulphuric acid solution. *Corros. Sci.*, **2011**, *53* (9), 2902-2913. https://doi.org/10.1016/j.corsci.2011.05.027.

[3] Döner, A.; Kardaş, G., N-Aminorhodanine as an effective corrosion inhibitor for mild steel in 0.5 M H_2SO_4. *Corros. Sci.*, **2011**, *53* (12), 4223-4232. https://doi.org/10.1016/j.corsci.2011.08.032.

[4] Thakur, A.; Kumar, A.; Sharma, S.; Ganjoo, R.; Assad, H., Computational and experimental studies on the efficiency of Sonchus arvensis as green corrosion inhibitor for mild steel in 0.5 M HCl solution. *Mater. Today Proc.*, **2022**, *66*, 609-621. https://doi.org/10.1016/j.matpr.2022.06.479.

[5] Padhan, S.; Rout, T. K.; Nair, U. G., N-doped and Cu, N-doped carbon dots as corrosion inhibitor for mild steel corrosion in acid medium. *Colloids Surfaces A Physicochem. Eng. Asp.*, **2022**, *653*, 129905. https://doi.org/10.1016/j.colsurfa.2022.129905.

[6] Thakur, A.; Kaya, S.; Abousalem, A. S.; Kumar, A., Experimental, DFT and MC simulation analysis of Vicia Sativa weed aerial extract as sustainable and eco-benign corrosion inhibitor for mild steel in acidic environment. *Sustain. Chem. Pharm.*, **2022**, *29*, 100785. https://doi.org/10.1016/j.scp.2022.100785.

[7] Thakur, A.; Kaya, S.; Abousalem, A. S.; Sharma, S.; Ganjoo, R.; Assad, H.; Kumar, A., Computational and experimental studies on the corrosion inhibition performance of an aerial extract of Cnicus Benedictus weed on the acidic corrosion of mild steel. *Process Saf. Environ. Prot.*, **2022**, *161*, 801-818. https://doi.org/10.1016/j.psep.2022.03.082.

[8] Fan, B.; Zhao, X.; Liu, Z.; Xiang, Y.; Zheng, X., Inter-component synergetic corrosion inhibition mechanism of Passiflora edulia Sims shell extract for mild steel in pickling solution: Experimental, DFT and reactive dynamics investigations. *Sustain. Chem. Pharm.*, **2022**, *29*, 100821. https://doi.org/10.1016/j.scp.2022.100821.

[9] Omran, M. A.; Fawzy, M.; Mahmoud, A. E. D.; Abdullatef, O. A., Optimization of mild steel corrosion inhibition by water hyacinth and common reed extracts in acid media using factorial experimental design. *Green Chem. Lett. Rev.*, **2022**, *15* (1), 216-232. https://doi.org/10.1080/17518253.2022.2032844.

[10] Chauhan, L. R.; Gunasekaran, G., Corrosion inhibition of mild steel by plant extract in dilute HCl medium.

Corros. Sci., **2007**, *49* (3), 1143-1161. https://doi.org/10.1016/j.corsci.2006.08.012.

[11] Patel, N. S.; Jauhariand, S.; Mehta, G. N.; Al-Deyab, S. S.; Warad, I.; Hammouti, B., Mild steel corrosion inhibition by various plant extracts in 0.5 M sulphuric acid. *Int. J. Electrochem. Sci.*, **2013**, *8* (2), 2635-2655. https://doi.org/10.1016/S1452-3981(23)14337-9.

[12] Ashassi-Sorkhabi, H.; Moradi-Alavian, S.; Esrafili, M. D.; Kazempour, A., Hybrid sol-gel coatings based on silanes-amino acids for corrosion protection of AZ91 magnesium alloy: Electrochemical and DFT insights. *Prog. Org. Coatings*, **2019**, *131*. https://doi.org/10.1016/j.porgcoat.2019.01.052.

[13] Ashassi-Sorkhabi, H.; Kazempour, A., Thermodynamic and kinetic insights into the role of amino acids in improving the adhesion of iota-carrageenan as a natural corrosion inhibitor to the aluminum surface. *J. Adhes. Sci. Technol.*, **2020**, *34* (9), 961-975. https://doi.org/10.1080/01694243.2019.1690776.

[14] Ashassi-Sorkhabi, H.; Kazempour, A.; Moradi-Alavian, S.; Asghari, E.; Vinodh, R.; Pollet, B. G. G., Electrodes Derived From Conducting Polymers and their Composites for Catalytic Conversion of Carbon Dioxide. *J. Electrochem. Soc.*, **2022**. https://doi.org/10.1149/1945-7111/aca830.

[15] Mirzaei-Saatlo, M.; Jamali, H.; Moradi-Alavian, S.; Asghari, E.; Teimuri-Mofrad, R.; Esrafili, M. D., 4-Ferrocenylbutyl-based corrosion inhibitors for mild steel in acidic solution. *Mater. Chem. Phys.*, **2023**, *293*, 126895. https://doi.org/10.1016/j.matchemphys.2022.126895.

[16] Cherrak, K.; Khamaysa, O. M. A.; Bidi, H.; El Massaoudi, M.; Ali, I. A.; Radi, S.; El Ouadi, Y.; El-Hajjaji, F.; Zarrouk, A.; Dafali, A., Performance evaluation of newly synthetized bi-pyrazole derivatives as corrosion inhibitors for mild steel in acid environment. *J. Mol. Struct.*, **2022**, *1261*, 132925. https://doi.org/10.1016/j.molstruc.2022.132925.

[17] El Azzouzi, M.; Azzaoui, K.; Warad, I.; Hammouti, B.; Shityakov, S.; Sabbahi, R.; Saoiabi, S.; Youssoufi, M. H.; Akartasse, N.; Jodeh, S., Moroccan, Mauritania, and senegalese gum Arabic variants as green corrosion inhibitors for mild steel in HCl: Weight loss, electrochemical, AFM and XPS studies.

J. Mol. Liq., **2022**, *347*, 118354. https://doi.org/10.1016/j.molliq.2021.118354.

[18] Nahlé, A.; Salim, R.; Hajjaji, F. E. L.; Ech-chihbi, E.; Titi, A.; Messali, M.; Kaya, S.; El Ibrahimi, B.; Taleb, M., Experimental and theoretical approach for novel imidazolium ionic liquids as Smart Corrosion inhibitors for mild steel in 1.0 M hydrochloric acid. *Arab. J. Chem.*, **2022**, *15* (8), 103967. https://doi.org/10.1016/j.arabjc.2022.103967.

[19] Al-Amiery, A. A.; Mohamad, A. B.; Kadhum, A. A. H.; Shaker, L. M.; Isahak, W. N. R. W.; Takriff, M. S., Experimental and theoretical study on the corrosion inhibition of mild steel by nonanedioic acid derivative in hydrochloric acid solution. *Sci. Rep.*, **2022**, *12* (1), 1-21. https://doi.org/10.1038/s41598-022-08146-8.

[20] Melhi, S.; Bedair, M. A.; Alosaimi, E. H.; Younes, A. A. O.; El-Shwiniy, W. H.; Abuelela, A. M., Effective corrosion inhibition of mild steel in hydrochloric acid by newly synthesized Schiff base nano Co(ii) and Cr(iii) complexes: spectral, thermal, electrochemical and DFT (FMO, NBO) studies. *RSC Adv.*, **2022**, *12* (50), 32488-32507. https://doi.org/10.1039/D2RA06571A.

[21] Mahdi, B. S.; Abbass, M. K.; Mohsin, M. K.; Al-Azzawi, W. K.; Hanoon, M. M.; Al-Kaabi, M. H. H.; Shaker, L. M.; Al-Amiery, A. A.; Isahak, W. N. R. W.; Kadhum, A. A. H., Corrosion inhibition of mild steel in hydrochloric acid environment using terephthaldehyde based on Schiff base: Gravimetric, thermodynamic, and computational studies. *Molecules*, **2022**, *27* (15), 4857. https://doi.org/10.3390/molecules27154857.

[22] Sharma, S.; Ganjoo, R.; Kr. Saha, S.; Kang, N.; Thakur, A.; Assad, H.; Sharma, V.; Kumar, A., Experimental and theoretical analysis of baclofen as a potential corrosion inhibitor for mild steel surface in HCl medium. *J. Adhes. Sci. Technol.*, **2022**, *36* (19), 2067-2092. https://doi.org/10.1080/01694243.2021.2000230.

[23] Daoudi, W.; El Aatiaoui, A.; Falil, N.; Azzouzi, M.; Berisha, A.; Olasunkanmi, L. O.; Dagdag, O.; Ebenso, E. E.; Koudad, M.; Aouinti, A., Essential oil of Dysphania ambrosioides as a green corrosion inhibitor for mild steel in HCl solution. *J. Mol. Liq.*, **2022**, *363*, 119839. https://doi.org/10.1016/j.molliq.2022.119839

[24] Ganjoo, R.; Sharma, S.; Thakur, A.; Assad, H.; Sharma, P. K.; Dagdag, O.; Berisha, A.; Seydou, M.; Ebenso,

E. E.; Kumar, A., Experimental and theoretical study of Sodium Cocoyl Glycinate as corrosion inhibitor for mild steel in hydrochloric acid medium. *J. Mol. Liq.*, **2022**, *364*, 119988. https://doi.org/10.1016/j.molliq.2022.119988.

[25] Cobá-Tec, E. Y.; Pech-Canul, M. A., Corrosion behavior and surface properties of mild steel in aqueous citrate solutions. *Chem. Eng. Commun.*, **2022**, 1-17. https://doi.org/10.1080/00986445.2022.2039914.

[26] Wang, X.; Yang, H.; Wang, F., An investigation of benzimidazole derivative as corrosion inhibitor for mild steel in different concentration HCl solutions. *Corros. Sci.*, **2011**, *53* (1), 113-121. https://doi.org/10.1016/j.corsci.2010.09.029.

[27] Verma, C.; Thakur, A.; Ganjoo, R.; Sharma, S.; Assad, H.; Kumar, A.; Quraishi, M. A.; Alfantazi, A., Coordination bonding and corrosion inhibition potential of nitrogen-rich heterocycles: Azoles and triazines as specific examples. *Coord. Chem. Rev.*, **2023**, *488*, 215177. https://doi.org/10.1016/j.ccr.2023.215177.

[28] Yeganeh, M.; Saremi, M.; Rezaeyan, H., Corrosion inhibition of steel using mesoporous silica nanocontainers incorporated in the polypyrrole. *Prog. Org. Coatings*, **2014**, *77* (9), 1428-1435. https://doi.org/10.1016/j.porgcoat.2014.05.007.

[29] Kong, P.; Feng, H.; Chen, N.; Lu, Y.; Li, S.; Wang, P., Polyaniline/chitosan as a corrosion inhibitor for mild steel in acidic medium. *RSC Adv.*, **2019**, *9* (16), 9211-9217. https://doi.org/10.1039/C9RA00029A.

[30] Pereira, S. S. de A. A.; Pêgas, M. M.; Fernández, T. L.; Magalhães, M.; Schöntag, T. G.; Lago, D. C.; de Senna, L. F.; D'Elia, E., Inhibitory action of aqueous garlic peel extract on the corrosion of carbon steel in HCl solution. *Corros. Sci.*, **2012**, *65*, 360-366. https://doi.org/10.1016/j.corsci.2012.08.038.

[31] Ashassi-Sorkhabi, H.; Kazempour, A.; Frouzat, Z., Superior potentials of hydrazone Schiff bases for efficient corrosion protection of mild steel in 1.0 M HCl. *J. Adhes. Sci. Technol.*, **2021**, *35* (2), 164-184. https://doi.org/10.1080/01694243.2020.1794357.